

# Spatiotemporal characteristics of cerebral blood volume changes in rat somatosensory cortex evoked by sciatic nerve stimulation and obtained by optical imaging

Pengcheng Li  
Qingming Luo  
Weihua Luo  
Shangbin Chen  
Haiying Cheng  
Shaoqun Zeng

Huazhong University of Science and Technology  
Key Laboratory of Biomedical Photonics of the  
Ministry of Education  
Wuhan, 430074  
Hubei, People's Republic of China  
E-mail: ibp@mail.hust.edu.cn

**Abstract.** The spatiotemporal characteristics of changes in cerebral blood volume associated with neuronal activity were investigated in the hindlimb somatosensory cortex of  $\alpha$ -chloralose-urethane anesthetized rats ( $n=10$ ) with optical imaging at 570 nm through a thinned skull. Activation of the cortex was carried out by electrical stimulation of the contralateral sciatic nerve with 5-Hz, 0.3-V pulses (0.5 ms) for 2 s. The stimulation evoked a monophasic decrease in optical reflectance at the cortical parenchyma and arterial sites soon after the onset of stimulation, whereas no similar response was observed at vein compartments. The optical signal changes reached 10% of the peak response  $0.70\pm 0.32$  s after the start of stimulation, and no significant time lag in this 10% start latency time was observed between the response at the cortical parenchyma and artery compartments. The decrease in optical reflectance reached a peak ( $0.25\pm 0.047\%$ )  $2.66\pm 0.61$  s after stimulus onset at parenchymal sites, which is  $0.40\pm 0.20$  s earlier ( $P<0.05$ ) than that at arterial sites ( $0.50\pm 0.068\%$   $3.06\pm 0.70$  s). Varying the locations within the cortical parenchyma and arterial compartments did not significantly affect the temporal characteristics of the evoked signal. These results suggest that stimulation of the sciatic nerve evokes an increase in local blood volume in both capillaries (cortical parenchyma) and arterioles soon after the onset of a stimulus, but the blood volume increase evoked in capillaries could not be entirely accounted for by the dilation of arterioles. © 2003 Society of Photo-Optical Instrumentation Engineers. [DOI: 10.1117/1.1609199]

Keywords: sciatic nerve stimulation; rat hindlimb somatosensory cortex; optical imaging; cerebral blood volume.

Paper 02074 received Oct. 23, 2002; revised manuscript received Mar. 19, 2003; accepted for publication Apr. 4, 2003.

## 1 Introduction

It is well known that there is a tight coupling between changes in electrical activity in the brain and responses of the microcirculation.<sup>1,2</sup> Although this coupling is used by neuroimaging techniques to visualize the neuronal electrical activity indirectly in living brain, such as positron emission tomography (PET), optical imaging based on intrinsic signal, and functional magnetic resonance imaging (fMRI), the dynamics of neurovascular coupling and the underlying mechanism of vascular regulation are not yet fully understood. There are two possible locations in the vascular compartment where the initial activity-evoked microcirculatory regulation cause take place: arterioles and capillaries.<sup>3</sup>

By tracking pial arteriolar diameter during 20 s of sciatic nerve stimulation in the rat, Ngai et al.<sup>4</sup> observed a dilation of pial arterioles in the hindlimb sensory cortex.<sup>4</sup> Using laser Doppler flowmetry (LDF), they subsequently showed that dilation of surface arterioles was accompanied by a local increase in cerebral perfusion.<sup>5</sup> Matsuura et al.<sup>3</sup> used LDF to measure the changes in red blood cell (RBC) velocity and concentration independently during activation of rat somatosensory cortex by direct microelectrical stimulation, and no significant time lag in the latency between RBC velocity and

concentration was observed, which suggests that both arteriolar dilation and capillary volume change contribute simultaneously to the initial regulation of local cerebral blood flow (CBF).<sup>6</sup>

Malonek et al.<sup>6</sup> reported their results with LDF and imaging spectroscopy studies in the cat visual cortex, which showed that the stimulation-evoked changes in cerebral blood volume (CBV) displayed an apparent similarity with the CBF-LDF curves but preceded the CBF increase by about 1 s. They thus supposed that the capillary change might occur before arteriolar dilation. However, the LDF used in these experiments had low spatial resolution (the sample volume was estimated to be approximately  $1\text{ mm}^3$ ) and only an integrated CBF change was measured.<sup>3,6</sup> Although the improved LDF monitors the RBC velocity and concentration independently, no detailed behavioral image of different microvascular compartments, such as venules, arterioles, and capillaries in parenchyma, during cortical activation evoked by the sensory stimulation was provided separately.<sup>3</sup>

Nuran and Lauritzen<sup>7</sup> examined the contribution of single vascular elements to the local increase of CBF accompanying

the increased neuron activity in response to electrical stimulation of parallel and climbing fibers by using scanning laser Doppler flowmetry (SLDF). The high spatial resolution ( $\sim 5 \mu\text{m}$ ) applied in their studies enabled them to investigate the flow changes in arterioles, venules, and small vessels separately. But the 2-s temporal resolution of SLDF limited its application for observing the initial phase of neurovascular coupling.

To explore the possible location of the vasculature where microcirculation is initially regulated, it is necessary to obtain spatiotemporal activity-dependent vascular-response images with high resolution around the sites where the electrical recordings are targeted. The intrinsic optical imaging technique has achieved a two-dimensional spatial resolution of 20 to  $100 \mu\text{m}$  and a temporal resolution of milliseconds, which has been used to approximate local blood volume changes at the hemoglobin-isosbestic wavelength (570 nm) and reveal Hb changes at 605 nm during sensory stimulation.<sup>8</sup> Therefore optical imaging may shed light on the spatiotemporal dynamics of microvascular regulation and mechanisms controlling this local interaction. However, based on the finding that the early increase in the deoxyhemoglobin concentration starting less than 100 ms after the onset of stimulation is highly collocated with electrical activity at the columnar level whereas the delayed (300 ms after the onset of stimulation) increase in blood volume is not,<sup>9</sup> studies using optical imaging of an intrinsic signal mainly focused on visualizing the functional architecture at the level of individual cortical columns such as the orientation columns of the visual cortex in cat and monkey<sup>9,10</sup> and the single whisker functional representation in the rat barrel cortex,<sup>11,12</sup> and regarded the blood vessel response observed as an artifact.<sup>8</sup> There have been a few attempts to give the spatiotemporal characteristics of the vascular response evoked by peripheral nerve stimulation.<sup>10,11,13,14</sup> However, details on the statistical estimation of the timing of CBV changes in different microvascular compartments have not been fully provided. In the present study, optical reflectance recording at 570 nm was performed to obtain a detailed estimate of the spatiotemporal characteristics of blood volume changes, such as the start latency, peak latency, termination time, and peak amplitude, in different microcirculation compartments (cortical parenchyma, where capillaries are embedded, and in arteries and veins), in response to 2-s electrical stimulation of the sciatic nerve, and to help in understanding the dynamics of neurovascular coupling.

## 2 Materials and Methods

### 2.1 Animal Preparation

Adult male Wistar rats weighing between 300 and 400 g were anesthetized with an intraperitoneal injection of  $\alpha$ -chloralose and urethane (50 and 600 mg/kg, respectively). After tracheotomy, artificial ventilation was started using a small rodent ventilator (TKR-2000C, China). The body temperature was monitored with a rectal probe and maintained at  $37.0 \pm 0.5^\circ\text{C}$  using a heating regulator pad. The femoral artery and vein were cannulated to record arterial blood pressure and infusion of saline, respectively. The arterial  $\text{pO}_2$ ,  $\text{pCO}_2$ , and pH were measured periodically. The rats were fixed in a stereotactic frame and the parietal bone overlying the rat hindlimb somatosensory cortex was thinned to translucency with a saline-

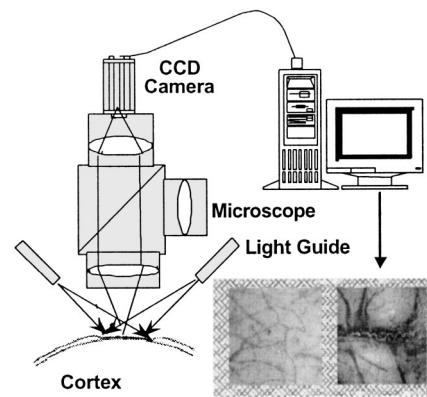


Fig. 1 Schematic drawing of optical imaging setup.

cooled dental drill to form a “window” over an area  $4 \times 4 \text{ mm}^2$ , centered 2 mm caudally and 2 mm laterally to the bregma, respectively. A plastic chamber was placed over the “window,” attached to the skull with dental cement, and then filled with silicon oil. The contralateral sciatic nerve was dissected free, placed on a pair of stimulating electrodes, and bathed in a pool of warm mineral oil. The measurements were performed at least 30 min after the surgical preparation to ensure a stable condition of the animal.

### 2.2 Sciatic Nerve Stimulation

Electrical stimulation of the sciatic nerve using rectangular pulses (0.5 ms) was applied at the rate of 5 Hz for 2 s, and the intensity of the stimulus was adjusted to be above the twitch threshold ( $\sim 0.3 \text{ V}$ ). The stimulation was given at 1-min intervals for fifteen trials and both stimulus intensity and frequency were kept constant throughout the experiment.

### 2.3 Measurement of Evoked Potential

An Ag-AgCl electrode was placed on the surface of the somatosensory cortex of the hindlimb area through the thinned portion of the skull. We detected the proper position of the maximal somatosensory-evoked potentials (SEPs) signal with short latency ( $\sim 10 \text{ ms}$ ) during stimulations as an indicator of the position of the activated cortex. The reference electrode was inserted into the scalp, and the ground lead was attached to an ear bar. The stimulations were generated by the SEP recording system.

### 2.4 Optical Imaging

On each trial, the images of backscattered and reflected light were collected and stored in the random-access memory (RAM) of a computer over a 9-s period at 40 Hz using a 12-bit  $640 \times 480$  pixels video camera (PixelFly VGA, Germany) attached to a microscope (Olympus SZ6045TRCTV, Japan). After the acquisition of all 360 frame images was completed, the images were transferred from RAM to the hard disk. Frames were recorded 1 s before the start of stimulation. The stimulations were generated with a stimulator (STG1004, Germany) and the stimulator was triggered by the CCD busy output signal of the CCD camera. The rat hindlimb somatosensory cortex was illuminated with light at 570 nm through a dual light guide (Olympus LG-DI, Japan) (for optical imaging setup, see Fig. 1). No dark-field method was used in our

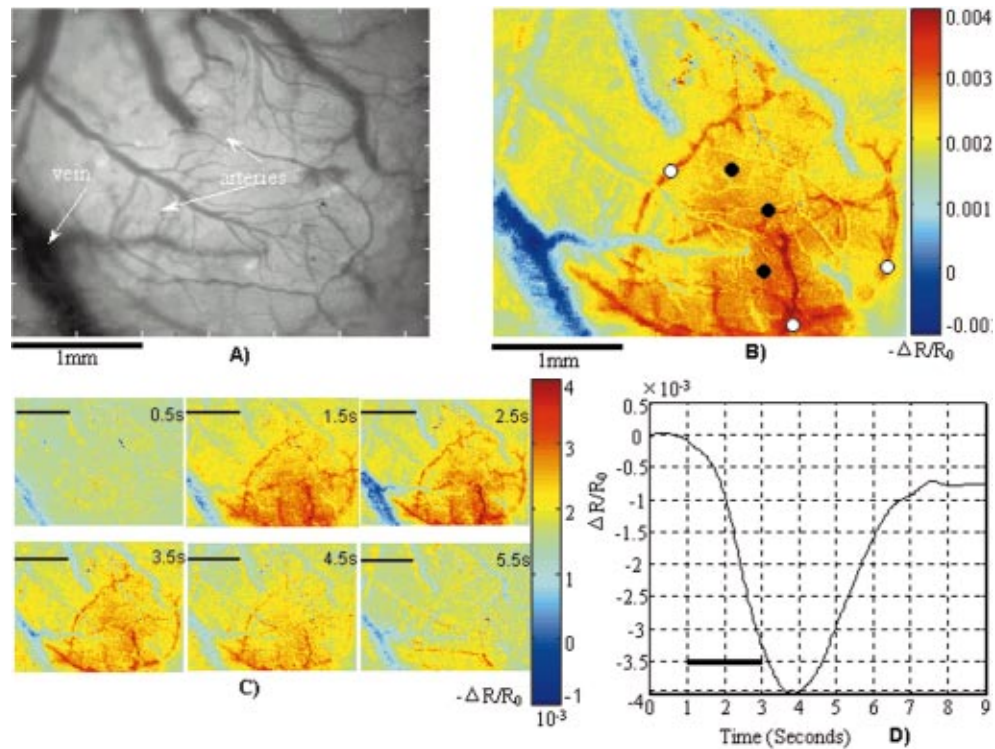


**Fig. 2** Spatial pattern of stimulus-induced optical reflectance changes ( $\Delta R/R_0$ ) at 570 nm. (a) Raw image of exposed rat cortex through a thinned skull at 570 nm illumination. The parietal branches of the superior cerebral vein and arteries are clearly distinguishable. (b) The spatial pattern of a stimulation-evoked vascular response. White circles indicate arteries, black dots indicate cortical parenchyma. The image was obtained by averaging the activation maps from 2.5 to 3 s after the onset of stimulation. The activation map was a visualization of the optical reflectance difference between an individual frame after stimulus onset and the mean intensity of frames prior to the stimulation. The color bar indicates the amplitude of signal change  $\Delta R/R_0$ , where  $R$  = optical reflectance collected during an individual image and  $\Delta R = R_i - R_0$  denotes the reflectance difference between frame  $i$ 'th and the baseline level. (c) Time course of activation maps in one experimental animal. Among the top images, the left, middle, and right images correspond, respectively, to mean activation maps during 0.5 s (averaged from 0 to 0.5 s), 1.5 s (averaged from 1 to 1.5 s), and 2.5 s (averaged from 2 to 2.5 s). The left, middle, and right images shown at bottom correspond, respectively, to mean activation maps during 3.5 s (averaged from 3 to 3.5 s), 4.5 s (averaged from 4 to 4.5 s) and 5.5 s (averaged from 5 to 5.5 s). (d) Mean temporal response of optical reflectance changes over the entire activated region across animals ( $n=10$ ). The horizontal bar in the chart indicates the duration of stimulation.

optical imaging studies. The two-dimensional optical spatial resolution and time resolution applied in these optical imaging studies were  $5 \mu\text{m}/\text{pixel}$  (over a  $3.2 \times 2.4\text{-mm}$  field) and 25 ms, respectively.

### 2.5 Data Analysis of Optical Imaging

The images were processed with the so-called “first frame analysis” in which the first frame was subtracted from all the subsequent frames before any further analysis was done. In order to correct the uneven illumination, all the image frames were divided by the first frame data. Then the data were averaged over the fifteen trials on a frame-by-frame basis to remove the 0.1-Hz low frequency oscillatory noise caused by cerebral vasomotion.<sup>15</sup> The temporal course of the evoked changes in optical signal was calculated as the mean value of the optical intensity changes in all the pixels within the region of activated cortex. The region of activated cortex was determined as the position where the surface SEPs signal can be detected. The time courses of the reflectance changes evoked by the sciatic stimulation were processed with a zero phase-shift digital low-pass filter with the cutoff frequency set to 1 Hz to remove the noise induced by heart beats and respiration and averaged over the animals used. The light at 570 nm is at a hemoglobin-isosbestic wavelength and was used to approximate blood volume changes in response to sensory stimulation in previous studies.<sup>6,8,10,15</sup> Here we ignored the effect of light scattering changes that may be induced by the stimulation and assumed that the absorption change was dominated by the contribution of only two chromophores—oxyhemoglobin and deoxyhemoglobin—when we calculated the blood volume change from the reflectance measurement. According to the modified Beer-Lambert law, the light intensity after absorption and scattering of tissue at a given wavelength can be expressed by

$$OD = -\log_{10}(R/R_0) = \sum_i \varepsilon_i C_i L = \varepsilon_{\text{Hb}} C_{\text{Hb}} L + \varepsilon_{\text{HbO}_2} C_{\text{HbO}_2} L, \quad (1)$$

where  $R$  is the reflected light intensity,  $R_0$  is the incident intensity,  $C$  is the concentration of the absorbing molecules (in molar),  $\varepsilon$  is the molar extinction coefficient (in  $\text{molar}^{-1} \text{mm}^{-1}$ ) at the selected wavelength, and  $L$  is the path length (in molar). So the relative changes in total hemoglobin (HbT) concentration from baseline can be obtained by

$$\begin{aligned} \Delta C_{\text{HbT}} &= \Delta C_{\text{Hb}} + \Delta C_{\text{HbO}_2} = \frac{\Delta OD}{\varepsilon_{\text{Hb}}^{570 \text{ nm}} L} \\ &= \frac{-\log_{10}(R_{\text{sti}}/R_{\text{baseline}})}{\varepsilon_{\text{Hb}}^{570 \text{ nm}} L}. \end{aligned} \quad (2)$$

We choose 1 mm as the path length, which was suggested by the Monte Carlo simulation experiments in the literature.<sup>16,17</sup> The parameters used for depicting the temporal characteristics of the response included start latency, peak latency, termination time, and peak amplitude. The start latency was determined as the time to reach 10% of the maxim evoked change in reflectance after the onset of stimulation, and the termina-

tion time was the time elapsed until the reflectance returned to the baseline level after stimulation. Peak latency was the time to reach maximum changes after stimulus onset. An analysis of variance (ANOVA) was used to compare the peak amplitude, peak latency, and termination time of the optical signal changes evoked in different microvascular compartments. The values were considered statistically significant at  $P < 0.05$ . All data were expressed as mean  $\pm$  S.D.

## 3 Results

The results shown here are based on experiments performed in ten male Wistar rats. The mean arterial blood pressure (MABP) and blood gas values of all ten animals were as follows: MABP =  $115.2 \pm 9.3$  mm Hg,  $p\text{O}_2 = 125.5 \pm 14$  mm Hg,  $p\text{CO}_2 = 37.2 \pm 3.6$  mm Hg, and  $\text{pH} = 7.4 \pm 0.06$ . The values were maintained within a stable range throughout each experiment. The arterial blood pressure did not change significantly during the stimulation.

### 3.1 Spatial Pattern of Evoked CBV Changes: Cortical Parenchyma, Arterioles, and Veins

In Fig. 2(a) the raw CCD image of the exposed cortex illuminated with 570-nm light clearly shows the anatomical cerebral vascular pattern through a thinned skull. In each rat, electrical stimulation of the sciatic nerve evoked a monophasic decrease in the optical reflectance of 570 nm at a location centered 2 mm laterally and caudally to the bregma, which was consistent with the hindlimb projection area of the somatosensory cortex. A decrease in the optical reflectance with 570-nm light indicated an increase in evoked local blood volume (under the assumption that the hematocrit remains constant) at the activated cortex. This increase in blood volume peaked at about 3 s and returned to the baseline about 7 s after the stimulus onset [see Fig. 2(d)]. As shown in Fig. 2(b) the vascular response evoked by sciatic nerve stimulation was found only in the arteries and the cortical parenchyma compartments where capillaries are embedded. No such stimulus-dependent blood volume increase during sciatic nerve stimulation was observed in the large cortical vein sites in our studies. All ten experimental animals exhibited a similar spatial response.

### 3.2 Temporal Pattern of Evoked CBV Changes

#### 3.2.1 Mean temporal pattern over entire activated region

The evoked change in reflectance started to decrease rapidly after the onset of stimulus and kept decreasing until it peaked at  $2.85 \pm 0.66$  s and returned to the baseline level  $6.60 \pm 0.45$  s after the onset of stimulation [see Fig. 2(d)]. The mean amplitude of the peak of optical signal changes evoked by the 5-Hz, 2-s electrical sciatic nerve stimulus was  $0.38 \pm 0.18\%$  over the activated region, including both cortical parenchyma and arteries.

#### 3.2.2 Difference of temporal dynamics of CBV changes evoked at different vascular compartments

In order to investigate the temporal dynamics of the local blood volume changes evoked at different vascular compartments, six small regions (each  $0.1 \times 0.1$  mm) were selected for analysis. The region of interest was determined in the follow-

**Table 1** Temporal characteristics of optical reflectance changes in somatosensory cortex evoked by sciatic nerve stimulation.

	Peak Amplitude (%)	Start Latency (seconds)	Peak Latency (seconds)	Termination Time (seconds)
Cortical parenchyma	$0.25 \pm 0.047$	$0.70 \pm 0.32$	$2.66 \pm 0.61$	$5.90 \pm 1.20$
Arteries	$0.50 \pm 0.068$		$3.06 \pm 0.70$	$6.70 \pm 1.30$

ing manner: (1) three  $0.01\text{-mm}^2$  regions were selected in the parenchyma compartment and in the arterial compartment, denoted by black and white circles, respectively [see Fig. 2(b)]; (2) all the regions of interest were discrete and at least  $0.2\text{ mm}$  apart. The temporal responses of the changes in optical reflectance in the cortical parenchyma and arteries are summarized in Table 1. As shown in Fig. 3(a), the local changes in optical reflectance at both parenchymal and arterial sites exhibited a similar shape of a monophasic decrease. The normalized

$\Delta\text{CBV}$  started to increase rapidly after the stimulus onset and reached 10% of the peak response  $0.70 \pm 0.32\text{ s}$  after the onset of stimulation. There was no significant time lag in this 10% start latency time between parenchyma (capillaries) and arteries at the site of the activated cortex [see Fig. 3(b)]. However, there were significant differences in peak amplitude, peak latency, and termination time of the changes in optical signal between the parenchyma and the arterial compartment. At the parenchyma site, the stimulus-induced signal changes

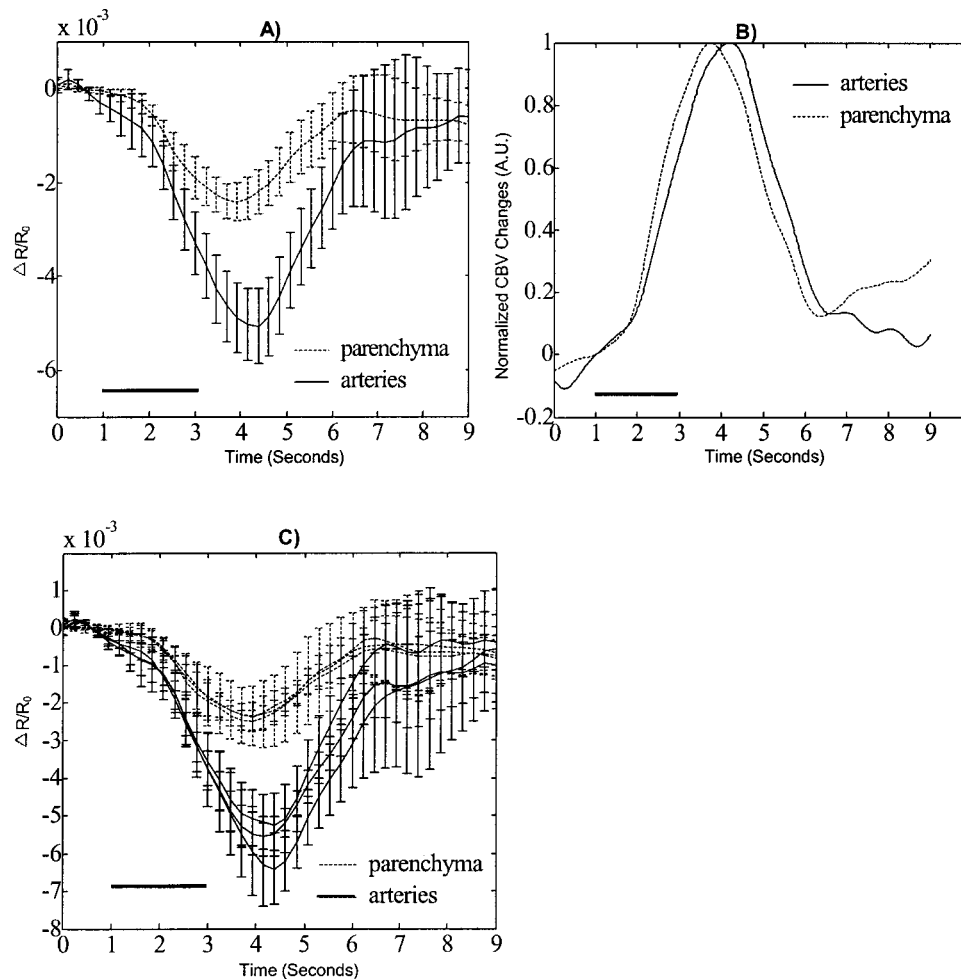


**Fig. 3** Time course of stimulus-evoked optical reflectance changes at 570 nm in different microvascular compartments across animals ( $n=10$ ) for the cortical parenchyma and arteries. The horizontal bars indicate the duration of stimulation. (a) Mean temporal dynamics over the regions indicated in Fig. 2(b). Both the parenchyma and artery plots are the average result of the time courses of their three  $0.01\text{-mm}^2$  "sampling" regions. (b) Normalized changes in blood volume regions indicated in Fig. 2(b). The blood volume changes were normalized to the peak amplitude of the signal changes. (c) Time courses of changes in optical reflectance in the six selected regions. Each plot results from averaging the intensity changes of all the pixels within the region of interest across ten experimental animals.

( $\Delta R/R_0$ , where  $\Delta R$  is the reflectance difference compared with that of the first frame and  $R_0$  is the optical reflection intensity of the first frame) reached their peak value of  $0.25 \pm 0.047\%$  at  $2.66 \pm 0.61$  s after the start of sciatic nerve stimulation and returned to baseline  $5.90 \pm 1.20$  s after stimulus onset. At arterial sites, the changes in optical signal reached their peak value of  $0.504 \pm 0.068\%$  at  $3.06 \pm 0.70$  s after stimulus onset and returned to the baseline  $6.70 \pm 1.30$  s after the onset. Further ANOVA statistical analysis showed that both peak amplitude and peak latency were significantly different in parenchymal and arterial sites [peak amplitude:  $F(1,58) = 17.30$ ,  $P < 0.01$ ; peak latency:  $F(1,58) = 5.41$ ,  $P < 0.05$ ]. The termination time of the optical signal changes in the two vascular compartments was also significantly different [ $F(1,58) = 5.595$ ,  $P < 0.05$ ]. However, varying the location within the parenchymal and arterial compartments themselves (the three regions sampled for parenchymal and artery sites, respectively) did not affect the peak amplitude, peak latency, and termination time significantly [see Fig. 3(c)].

#### 4 Discussion

Neuron activity initiates microcirculatory regulation. Using optical imaging spectroscopy<sup>18,19</sup> and laser-Doppler flowmetry,<sup>3,6,7,18</sup> the relationships between cerebral blood flow, oxygenation, and volume have been investigated on the rodent barrel cortex, the anesthetized cat, and the awake monkey. Focused on the initial phase of activation, some investigators observed a significant lag ( $\sim 1$  s) between blood volume and blood flow changes in cats and suggested that the increase in local blood volume prior to the increase in flow may result from an early functional recruitment of capillaries before the arteriolar segment dilates.<sup>6</sup> Myles et al.<sup>18</sup> obtained similar results in rodent studies but with a slight lag ( $\sim 0.2$  s) and the lag was just detectable with temporal resolution. Others found that there was no significant time lag in the latency between red blood cell velocity and concentration upon neuronal activation and suggested that both arteriole dilation and capillary volume changes contribute simultaneously to the initial regulation of CBF.<sup>3</sup>

In the present study, changes in local blood volume started to increase rapidly after the onset of the stimulus, which is consistent with the result of previous studies in cat visual cortex<sup>6</sup> and rat barrel cortex<sup>18</sup> using optical imaging spectroscopy. The signal change reached 10% of the peak response  $0.7 \pm 0.32$  s after the stimulus. There was no significant time lag in this 10% start latency time between parenchymal (capillaries) and arterial compartments at the activation site [see Fig. 3(b)]. This result suggests that the stimulus evokes a rapid increase in local blood volume in both capillaries and arterioles. The initial increase in capillaries may result from their functional recruitment, as suggested in Refs. 6 and 7, but the mechanism controlling the increase in blood volume (HbT concentration) in arterioles during this early phase is unclear. One possibility is that an activity-induced dilation of arterioles occurs, together with an independent increase in blood volume in capillaries. Although it has been reported that a prolonged (20 s) electrical stimulation of the sciatic nerve evoked a pial arteriole dilation after an initial brief latent period ( $< 2$  s)<sup>20</sup> and the prolonged (20 s) stimulation of parallel

fibers also produced arteriolar dilation,<sup>16</sup> the diameter changes in pial arterioles in response to short (2 s) stimulations requires further investigation.

As shown in Fig. 3(b), after reaching 10% of the peak response, the blood volume increases at two microvascular compartments diverged. The changes in the parenchyma compartment peaked  $2.66 \pm 0.61$  s after the onset of the stimulus, which is,  $0.4 \pm 0.2$  s before the change at an arterial site ( $P < 0.05$ ). This difference in the time-lag of peak latency indicates a faster increase in blood volume in capillaries than in arterioles, which suggests that the stimulus-induced increase in capillaries cannot be entirely accounted for by the dilation of arterioles.

In the present study, a decrease in optical reflectance induced by stimulation of the sciatic nerve occurred only at the arterial and parenchymal sites of the activated cortex, whereas no such response was observed in large cortical veins. The spatial pattern of vascular activities we observed is similar to that found by Nemoto et al.<sup>21</sup> at a similar region of the rat somatosensory cortex under 586-nm illumination during electrical stimulation of the hindlimb. Since both 570 nm and 586 nm are the isosbestic points of oxyhemoglobin and deoxyhemoglobin, the decreases in optical signal evoked by stimulation of the peripheral nerve are likely to indicate an activity-related increase in the concentration of total hemoglobin in arteries and capillaries.

However, at vein sites, although Narayan et al.<sup>13</sup> reported a functional venous optical signal with the stimulation of forelimb and whisker under both 550-nm (which is also a hemoglobin-isosbestic wavelength) and 605-nm light, our results are consistent with the findings of Nemoto et al.<sup>21</sup> and are supported by the observation of changes in the diameter of pial vessels during sciatic nerve stimulation in rats by Ngai et al.<sup>4,5</sup> In their studies, a dilation of pial arterioles in the hindlimb sensory cortex<sup>4</sup> and an accompanying increase in local cerebral blood flow<sup>5</sup> were detected during sciatic nerve stimulation, but no alteration in vein diameter was observed.<sup>4</sup> The absence of a decrease in optical reflectance under 570 nm in a large cortical vein during neuron activation indicates that no net change in the total hemoglobin concentration was evoked in veins, although the blood oxygenation in veins changes during cortex activation according to the results of optical imaging using 605 nm.

As shown in previous studies in the rat hindlimb (Nemoto et al.<sup>21</sup>), forelimb (Narayan et al.<sup>13</sup>), and barrel (Hess et al.,<sup>22</sup> Masino et al.,<sup>14</sup> Narayan et al.<sup>13</sup>) somatosensory cortex, an activity-related optical signal using 605 nm occurred at the cortical parenchyma and the draining cortical vein sites. Furthermore, the optical responses at this wavelength at the veins and parenchymal sites initially exhibited a biphasic pattern of decrease and then an increase in the optical reflectance. It is interesting that using another wavelength (577 nm), in which the extinction coefficient for oxyhemoglobin is only 1.67 times more than that for deoxyhemoglobin, Nemoto et al.<sup>21</sup> and Hess et al.<sup>22</sup> also reported the absence of a functional venous signal.

Based on the findings obtained with all these wavelengths, we arrived at the following picture of the dynamics of neurovascular coupling at veins: During the initial phase of neuron activation, there is an increase in deoxyhemoglobin and a decrease in oxyhemoglobin, but no net change in total hemo-

globin concentration, whereas during the later phase, oxyhemoglobin content increases and deoxyhemoglobin content decreases, with a roughly constant total hemoglobin content. The changes in blood oxygenation occurring at cortical vein sites could be a result of the venous drainage effect when the blood travels down the vascular tree from the site of activation.<sup>23</sup> Nemoto et al.<sup>21</sup> suggested that the absence of an optical signal decrease in veins during activation may be explained by the nonlinear relationship between the changes in concentrations of hemoglobin derivatives and the absorbance changes in the high absorbance range. However, this assumption may be questionable because of the existence of the optical signal at 605 nm.

## 5 Conclusion

The spatiotemporal characteristics of changes in local cerebral blood volume in the rat hindlimb somatosensory cortex evoked by electrical stimulation of the sciatic nerve were investigated by optical imaging at 570 nm. We statistically estimated the spatiotemporal characteristics of blood volume changes, such as the start latency, peak latency, termination time, and peak amplitude, in different microcirculation compartments (cortical parenchyma, arteries, and veins). Our results suggest that sciatic nerve stimulation evokes an increase in local blood volume in both arteries and cortical parenchyma sites soon after the onset of the stimulus, but that the blood volume increase in capillaries could not be entirely accounted for by the dilation of arterioles. However, we found no activity-related blood volume increase in large cortical veins.

## Acknowledgments

This work was supported by the National Science Fund for Distinguished Young Scholars (grant No. 60025514), the National Natural Sciences Foundation of China (30070215), and the National Basic Research Priorities Program (973) (Grant No. 2001CCA04100). Some of the results in this study have been presented in a paper in *Proc SPIE* **5068**.

## References

1. C. Roy and C. Sherrington, "On the regulation of the blood supply of the brain," *J. Physiol.* **11**, 85–108 (1890).
2. B. Chance, P. Cohen, F. Jobsis, and B. Schoener, "Intracellular oxidation-reduction states *in vivo*," *Science* **137**, 499–508 (1962).
3. T. Maturra, H. Fujita, C. Seki, C. K. Kashikura, and I. Kanno, "Hemodynamics evoked by microelectrical direct stimulation in rat somatosensory cortex," *Comp. Biochem. Physiol. A* **124**, 47–52 (1999).
4. A. C. Ngai, K. R. Ko, S. Morii, and H. R. Winn, "Effect of sciatic nerve stimulation on pial arterioles in rats," *Am. J. Physiol.* **254**(2), H133-9 (1988).
5. A. C. Ngai, J. R. Meno, and H. R. Winn, "Simultaneous measurements of pial arteriolar diameter and laser-Doppler flow during somatosensory stimulation," *J. Cereb. Blood Flow Metab.* **15**, 124–127 (1995).
6. D. Malonek, U. Dirnagl, U. Lindauer, K. Yamada, I. Kanno, and A. Grinvald, "Vascular imprints of neuronal activity: relationships between the dynamics of cortical blood flow, oxygenation, and volume

- changes following sensory stimulation," *Proc. Natl. Acad. Sci. U.S.A.* **94**, 14826–14831 (1997).
7. N. Akgören and M. Lauritzen, "Functional recruitment of red blood cells to rat brain microcirculation accompanying increased neuronal activity in cerebellar cortex," *NeuroReport* **10**, 3257–3263 (1999).
8. I. Vanzetta and A. Grinvald, "Evidence and lack of evidence for the initial dip in the anesthetized rat: implications for human functional brain imaging," *Neuroimage* **13**, 959–967 (2001).
9. D. Malonek and A. Grinvald, "Interaction between electrical activity and cortical microcirculation revealed by imaging spectroscopy: implications for functional brain mapping," *Science* **272**(5261), 551–554 (1996).
10. R. D. Frostig, E. E. Lieke, D. Y. Ts'o, and A. Grinvald, "Cortical functional architecture and local coupling between neuronal activity and the microcirculation revealed by *in vivo* high-resolution optical imaging of intrinsic signals," *Proc. Natl. Acad. Sci. U.S.A.* **87**, 6082–6086 (1990).
11. C. H. Chen-Bee, M. C. Kwon, S. A. Masino, and R. D. Frostig, "Areal extent quantification of functional representations using intrinsic signal optical imaging," *J. Neurosci. Methods* **68**, 27–37 (1996).
12. C. H. Chen-Bee, D. B. Polley, B. Brett-Green, M. C. Kwon, and R. D. Frostig, "Visualizing and quantifying evoked cortical activity assessed with intrinsic signal imaging," *J. Neurosci. Methods* **97**, 157–173 (2000).
13. S. M. Narayan, E. M. Santori, A. J. Blood, J. S. Burton, and A. W. Toga, "Imaging optical reflectance in rodent barrel and forelimb sensory cortex," *Neuroimage* **1**, 181–190 (1994).
14. S. A. Masino, M. C. Kwon, Y. Dory, and R. D. Frostig, "Characterization of functional organization within rat barrel cortex using intrinsic signal optical imaging through a thinned skull," *Proc. Natl. Acad. Sci. U.S.A.* **90**, 9998–10002 (1993).
15. J. Mayhew, S. Askew, Y. Zheng, J. Porril, G. Westby, P. Redgrave, D. Rector, and R. Happer, "Cerebral vasomotion: a 0.1-Hz oscillation in reflected light imaging of neural activity," *Neuroimage* **4**, 183–193 (1996).
16. J. Mayhew, Y. Zheng, Y. Hou, B. Wuksanovic, J. Berwick, S. Askew, and P. Coffey, "Spectroscopic analysis of changes in remitted illumination: the response to increased neural activity in brain," *Neuroimage* **10**, 304–326 (1999).
17. M. Kohl, U. Lindauer, G. Royl, M. Kühl, L. Gold, A. Villringer, and D. Dirnagl, "Physical model for the spectroscopic analysis of cortical intrinsic optical signals," *Phys. Med. Biol.* **45**, 3749–3764 (2000).
18. J. Myles, B. Jason, J. Dave, and J. Mayhew, "Concurrent optical imaging spectroscopy and laser-Doppler flowmetry: the relationship between blood flow, oxygenation, and volume in rodent barrel cortex," *Neuroimage* **13**, 1002–1015 (2001).
19. U. Lindauer, G. Royl, C. Leithner, M. Kühl, L. Gold, J. Gethmann, M. K. Bareis, A. Villringer, and U. Dirnagl, "No evidence for early decrease in blood oxygenation in rat whisker cortex in response to functional activation," *Neuroimage* **13**, 988–1001 (2001).
20. A. C. Ngai and H. R. Winn, "Pial arteriole dilation during somatosensory stimulation is not mediated by an increase in CSF metabolites," *Am. J. Physiol. Heart Circ. Physiol.* **282**, H902–H907 (2002).
21. M. Nemoto, Y. Nomura, C. Sato, M. Tamura, K. Houkin, I. Koyanagi, and H. Abe, "Analysis of optical signals evoked by peripheral nerve stimulation in rat somatosensory cortex: dynamic changes in hemoglobin concentration and oxygenation," *J. Cereb. Blood Flow Metab.* **19**, 246–259 (1999).
22. A. Hess, D. Stiller, T. Kaulisch, P. Heil, and H. Scheich, "New insights into the hemodynamic blood oxygenation level-dependent response through combination of functional magnetic resonance imaging and optical recording in gerbil barrel cortex," *J. Neurosci.* **20**(9), 3328–3338 (2000).
23. R. B. Buxton, "The elusive initial dip," *Neuroimage* **13**, 953–958 (2001).